ELSEVIER

Catalysis Today 69 (2001) 63–73

CATALYSIS TODAY

www.elsevier.com/locate/cattod

Simulation of structured catalytic reactors with enhanced thermal conductivity for selective oxidation reactions

Gianpiero Groppi, Enrico Tronconi*

Dipartimento di Chimica Industriale e Ingegneria Chimica "G. Natta", Politecnico di Milano, Piazza Leonardo da Vinci 32, 20133 Milano, Italy

Abstract

The replacement of conventional-packed beds of pellets with "high conductivity" honeycomb catalysts in industrial externally cooled multitubular fixed-bed reactors is investigated by modeling and simulation for the oxidation of methanol to formaldehyde and for the epoxidation of ethylene to ethylene oxide, which involve a consecutive and a parallel reaction scheme, respectively. Results suggest that near-isothermal operation of the fixed-bed reactors can be achieved using monolithic catalyst supports based on relatively large volume fractions of highly conductive materials. Pressure drops are reduced to less than 1%. The selectivity is favored by the excellent control of the intraporous diffusional resistances resulting from the thin catalytic washcoats. Reactor designs based on larger tubes are feasible at the expense of greater volume fractions of catalyst support. A critical aspect is represented by the restrictions on the specific load of catalyst per reactor volume resulting from the poor adhesion of very thick catalyst layers onto metallic surfaces. Such a difficulty can be circumvented by maximizing the geometric surface area of the monolith (e.g. minimizing the honeycomb pitch), enhancing the catalytic activity (e.g. increasing the load of active components), and increasing the coolant temperature (if the selectivity is not adversely affected).

Keywords: Fixed-bed reactors; Thermal conductivity; Oxidation reactions; Conductive monoliths

1. Introduction

Several advantages of monolithic and structured catalysts are well established, including, e.g. reduced pressure drops, easy scale-up, possibility to control intraporous diffusional resistances. Only recently, attention has been focused on one additional potential benefit offered by the connected solid matrix of monolithic supports, namely the exploitation of thermal conduction in addition to convection as an effective heat transfer mechanism.

In the previous works, we have investigated theoretically [1,2] and experimentally [3,4] the optimal design and the thermal behavior of structured catalysts with high thermal conductivity, in view of their use for strongly exothermic gas/solid reactions. The parametric analysis for the case of a single reaction [2] indicated that metallic honeycombs are promising for limiting temperature gradients in externally cooled multitubular fixed-bed reactors as compared to conventional packed beds of catalyst pellets. To take full advantage of heat conduction in the monolithic matrices, however, specific honeycomb designs must be developed which include relatively large volume fractions of support made of materials with a high intrinsic conductivity, as well as large loads of active

* Corresponding author. Tel.: +39-02-23993264; fax: +39-02-70638173.
E-mail address: enrico.tronconi@polimi.it (E. Tronconi).

0920-5861/01/$ – see front matter
PII: S0920-5861(01)00356-X

Nomenclature

c_p	mass specific heat (J/(kg K))
C	uniform dimensionless pressure downstream from the monolith, Eq. (10)
d_{eq}	$m\sqrt{\varepsilon}$, hydraulic diameter of the monolith channel (m)
D	external monolith diameter = inner reactor tube diameter (m)
D_k	mass diffusivity of the key species (m^2/s)
$D_{k,e}$	effective mass diffusivity of the key species in the washcoat (m^2/s)
Da^0	$D^2 MW_k R_1^0 / D_k \rho_g \omega_k^0$, Damkohler number
e	emissivity of solid phase
E_{act}	activation energy (J/mol)
f	friction factor
h	gas–solid heat transfer coefficient in the monolith channel (W/(m^2 K))
ΔH_r	reaction enthalpy (J/mol)
k	thermal conductivity (W/(m K))
$k_{e,ax}$	effective axial conductivity (W/(m K))
$k_{e,r}$	effective radial conductivity (W/(m K))
$k^*_{e,ax}$	$k_{e,ax}/k_s$, dimensionless effective axial conductivity
$k^*_{e,r}$	$k_{e,r}/k_s$, dimensionless effective radial conductivity
k^*_s	k_s/k_g, dimensionless solid conductivity
K_m	gas–solid mass transfer coefficient in the monolith channels (kg/(m^2 s))
L	monolith length (m)
L^*	L/D, dimensionless monolith length
Le	α/D_k, molecular Lewis number
m	monolith pitch (m)
m^*	m/D, dimensionless monolith pitch
M^0	$\rho_g^0 P^0 / W_t^2$
MW_k	molecular weight of key species (kg/kmol)
Nu	hd_{eq}/k_g, Nusselt number
P	pressure (Pa)
P^*	P/P^0, dimensionless pressure
Pr	$\mu_g c_{pg}/k_g$, Prandtl number
r	radial coordinate (m)
r^*	$2(r/D)$, dimensionless radial coordinate
R_j	rate of jth reaction (mol/(m^3 s))
R^*_j	R_j/R_j^0, dimensionless rate of jth reaction
Pe_m	$ReSc$, material Peclet number
Pe_T	$RePr$, thermal Peclet number
Re	$Wd_{eq}/\varepsilon\mu_g$, Reynolds number
Sc	$\mu_g/\rho_g D_k$, Schmidt number
Sh	$K_m d_{eq}/\rho_g D_k$, Sherwood number
T	temperature (K)
T^*	T/T_{cool}, dimensionless temperature
W	local specific mass flow rate (kg/(m^2 s))
W_t	mean specific mass flow rate, referred to the whole cross-section (kg/(m^2 s))
W^*	W/W_t, dimensionless specific mass flow rate at r^*
z	axial coordinate (m)
z^*	z/L, dimensionless axial coordinate

Greek symbols

α	thermal diffusivity (m^2/s)
β	$(-\Delta H_r)\omega_k^0 / T_{cool} c_p MW_k$, dimensionless adiabatic temperature rise
δ_w	$m(\sqrt{\varepsilon+\xi} - \sqrt{\varepsilon})$, thickness of active washcoat (m)
ε	monolith void fraction
η	$\tanh(\Phi)/\Phi$, effectiveness factor
λ	volume fraction of inert support
μ	viscosity (kg/(m s))
ξ	volume fraction of active phase
ρ_g	gas density (kg/m^3)
σ	$(T_{cool}^3 L\sigma_{SB} e/(\lambda k_s + \xi k_w))(\lambda+\xi)$
σ_{SB}	Stefan–Boltzmann constant (5.67E − 8 W/(m^2 K^4))
Φ_j	$\delta_w \sqrt{R_j MW_k / D_{k,e} \rho_g \omega_k}$, generalized Thiele modulus for jth reaction
ω_k	mass fraction of the key component
ω^*_k	ω_k/ω_k^0, normalized mass fraction

catalytic components. Such monolithic catalysts can be associated with effective radial thermal conductivities greater by one order of magnitude than in packed beds, but differ considerably from the existing conventional monoliths used in environmental catalysis [2].

An experimental study of home-made plate-type coated metallic catalysts in the oxidation of CO, taken as a model exothermic reaction, demonstrated that temperature gradients and hot-spot temperatures were drastically reduced when changing the support material from stainless steel to aluminum due to a tenfold

increment of the intrinsic metal conductivity [3,4]. The role of the support volume fraction was likewise evidenced, the data pointing out a significant decline of the temperature gradients when a support consisting of the same metal (stainless steel) with identical configuration but with a doubled thickness of the metal plates was adopted. In view of scale-up applications, it was also shown by experiment that essentially the same thermal behavior can be expected from plate-type catalysts with different geometrical configurations which share, however, the same volume fraction of solid support [4]. Altogether, the feasibility of running strongly exothermic reactions in a fixed-bed reactor under nearly isothermal conditions was experimentally confirmed on a general basis.

In this work, we proceed to explore by simulation the potential of "high conductivity" honeycomb catalysts in the operation of multitubular fixed-bed industrial reactors. Two important selective oxidation processes are considered in this respect, namely the partial oxidation of methanol to formaldehyde and the epoxidation of ethylene to ethylene oxide. In both such processes, secondary undesired reactions play a key role, i.e. the combustion of the primary product in the formaldehyde process, and the combustion of the ethylene reactant in the ethylene oxide process. Thus, the present study is intended to gain also indications on how the adoption of "high conductivity" monolith catalysts affects the selectivity of industrial partial oxidation processes for both a consecutive and a parallel reaction scheme.

2. Monolithic reactor model

2.1. Governing equations

Simulation results were generated by a steady-state pseudo-continuous heterogeneous 2D monolithic reactor model adapted from [2]. It describes a single externally cooled reactor tube loaded with a cylindrical honeycomb catalyst with square channels. The catalyst is represented as a continuum [1] consisting of a static, thermally connected solid phase (the inert support coated with a catalytic washcoat) and of a segregated gas phase in laminar flow inside the channels. The model equations include species mass balances and enthalpy balances for the gas and solid phases, as well as a momentum balance for the gas phase. Gas-phase concentration and temperature fields in the monolith channels are treated according to a 1D approximation, with gas–solid heat and mass transfer coefficients evaluated by analogy with the classical Graetz problem [5]. Intraporous diffusional limitations in the washcoat are accounted for by isothermal effectiveness factors based on the generalized Thiele modulus, and considering the consecutive or parallel nature of the reaction scheme. Additional major assumptions include: temperature-dependent gas properties; perfect thermal and mechanical contact between the honeycomb catalyst and the internal tube wall. Axial dispersion, gas-phase homogeneous reactions and radiative heat transfer (but for heat dispersion at the reactor inlet) are neglected. The model equations are presented in the following in dimensionless form, with symbols explained in Nomenclature.

Enthalpy balance, solid phase:

$$\frac{k^*_{e,ax}}{L^{*2}}\frac{\partial^2 T^*_s}{\partial z^{*2}} + 4k^*_{e,r}\left(\frac{\partial^2 T^*_s}{\partial r^{*2}} + \frac{1}{r^*}\frac{\partial T^*_s}{\partial r^*}\right) + \frac{4Nu}{k^*_s m^{*2}}(T^*_g - T^*_s) + \frac{Da^0}{k^*_s Le}\xi\sum_{j=1}^{NR}\beta_j\eta_j R^*_j = 0 \quad (1)$$

Key-species mass balance, solid phase:

$$\frac{4}{m^{*2}}Sh(\omega^*_{k,g} - \omega^*_{k,s}) + Da^0\xi\sum_{j=1}^{NR}\nu_{kj}\eta_j R^*_j = 0 \quad (2)$$

Enthalpy balance, gas phase:

$$\frac{Pe_t}{L^*}\frac{\partial T^*_g}{\partial z^*} + \frac{4}{m^{*2}}Nu(T^*_g - T^*_s) = 0 \quad (3)$$

Key-species mass balance, gas phase:

$$\frac{Pe_m}{L^*}\frac{\partial \omega^*_{k,g}}{\partial z^*} + \frac{4}{m^{*2}}Sh(\omega^*_{k,g} - \omega^*_{k,s}) = 0 \quad (4)$$

Momentum balance, gas phase:

$$\left(\frac{M^0}{W^{2*}}\varepsilon^2 - \frac{T^*_g}{P^{*2}}\right)\frac{\partial P^*}{\partial z^*} + \frac{1}{P^*}\frac{\partial T^*_g}{\partial z^*} + 2f\frac{L^*}{m^*\sqrt{\varepsilon}}\frac{T^*_g}{P^*} = 0 \quad (5)$$

Global mass balance:

$$2\int_0^1 W^* r^*\,\mathrm{d}r^* = 1 \quad (6)$$

Boundary conditions:

$$\text{Inlet conditions at } z^* = 0: \quad \frac{\partial T_s^*}{\partial z^*} = \sigma(T_s^{*4} - T_g^{0*4}) \tag{7a}$$

$$T_g^* = T_g^{0*}, \qquad \omega_{k,g}^* = 1 \tag{7b}$$

$$P^* = 1 - \frac{W^{*2} T_g^*}{2M^0 P^*} \tag{7c}$$

$$\text{Symmetry condition at } r^* = 0: \quad \frac{\partial T_s^*}{\partial r^*} = 0 \tag{8a}$$

$$\text{Boundary condition at } r^* = 1: \quad T_s^* = 1 \tag{8b}$$

$$k_{e,r} = k_s \left((1-\sqrt{\varepsilon+\xi}) + \frac{\sqrt{\varepsilon+\xi}-\sqrt{\varepsilon}}{(1-\sqrt{\varepsilon+\xi})+(k_w/k_s)\sqrt{\varepsilon+\xi}} + \frac{\sqrt{\varepsilon}}{(1-\sqrt{\varepsilon+\xi})+(k_w/k_s)(\sqrt{\varepsilon+\xi}-\sqrt{\varepsilon})+(k_g/k_s)\sqrt{\varepsilon}} \right)^{-1} \tag{12}$$

$$\text{Outlet condition at } z^* = 1: \quad \frac{\partial T_s^*}{\partial z^*} = 0 \tag{9}$$

Condition of uniform pressure downstream from the monolith:

$$\text{At } z^* = 1: \quad P^* - \frac{W^{*2} T_g^*}{2M^0 P^*} = C \tag{10}$$

Following Eigenberger [6], different thermal boundary conditions for the solid phase at the inlet and at the outlet of the reactor, respectively, accounting for radiative heat dispersion at the inlet, Eq. (7a), and assuming adiabatic termination at the outlet, Eq. (9), have been adopted. In Eqs. (7c) and (10), concentrated entrance and exit pressure losses are included as half of the kinetic head, however, their contribution was found practically negligible in all the cases.

2.1.1. Numerical methods

The set of coupled PDEs, Eqs. (1)–(10), was solved by orthogonal collocation techniques (for discretization of the dimensionless variable profiles along the radial coordinate of the monolith cross-section) [7], and by orthogonal collocation on finite elements [7] with an adaptive mesh algorithm [8] (for discretization of the variable profiles along the axial coordinate) in order to account for steep temperature gradients associated with the hot spots. The resulting system of 516 nonlinear algebraic equations was solved by a continuation method [9].

2.1.2. Heat transfer parameters

Axial and radial effective thermal conductivities appearing in Eq. (1), $k_{e,ax}$ and $k_{e,r}$, were estimated as functions of monolith geometry and material properties according to the following expressions, derived from a theoretical analysis of heat conduction in the unit square cell of a washcoated honeycomb catalyst [1,4]:

$$k_{e,ax} = k_s \left(\lambda + \frac{k_w}{k_s} \xi \right) \tag{11}$$

Eqs. (11) and (12) show that the effective conductivities $k_{e,r}$ and $k_{e,ax}$ are directly proportional to the intrinsic thermal conductivity of the support material, k_s. Therefore, heat transfer in monoliths is optimized by the adoption of highly conductive support materials, e.g. aluminum ($k_s \cong 200\,\mathrm{W/(m\,K)}$) is about 10 times better than FeCrAlloy ($k_s \cong 15$–$25\,\mathrm{W/(m\,K)}$) in this respect. Notably, even though aluminum is not suitable for such high temperature applications as catalytic combustors or catalytic mufflers, it can withstand the typical operating temperatures of most chemical catalytic processes. Aluminum is regarded as the support material of choice for the simulation studies herein reported.

In the following, the mathematical model of the monolithic reactor is applied to simulate multitubular, externally cooled fixed-bed reactors loaded with "high conductivity" monolith catalysts to carry out two strongly exothermic reactions of relevant industrial interest, namely the oxidation of methanol to formaldehyde and the epoxidation of ethylene.

3. Results and discussion

3.1. Oxidation of methanol to formaldehyde

We refer in this section to an industrial multitubular reactor loaded with metallic honeycomb monoliths

Table 1
Simulation parameters for the industrial formaldehyde reactor [10]

Reactor	
Tube length, L (m)	0.7
Tube inner diameter, D (m)	0.0266
Catalyst density, ρ_{cat} (kg/m^3)	2000
Operating conditions	
Mass velocity, W_t (kg/(m^2 s))	2.5
Inlet temperature, T^0 (°C)	250
Inlet pressure, P^0 (atm)	1.55
Feed CH_3OH mole fraction, $Y^0_{CH_3OH}$	0.05

coated with an industrial Fe_2O_3–MoO_3 catalyst for the selective oxidation of CH_3OH to HCHO. Kinetics, design and operating variables were derived from the extensive simulation work reported in [10], which provides also reference parameters for an optimized industrial packed-bed reactor. Notably, the reaction scheme is consecutive in this case

$$CH_3OH + \tfrac{1}{2}O_2 \rightarrow HCHO + H_2O, \quad \Delta H_R = -38\,\text{kcal/mol} \tag{13}$$

$$HCHO + \tfrac{1}{2}O_2 \rightarrow CO + H_2O, \quad \Delta H_R = -56\,\text{kcal/mol} \tag{14}$$

According to the rate expressions provided in [10], which reflect the original kinetic investigation of Dente et al. [11], the activation energy of the undesired HCHO oxidation to CO (16 kcal/mol) is lower than that of the primary partial oxidation of CH_3OH to HCHO (20 kcal/mol). Other relevant operating and design parameters are summarized in Table 1. In the industrial packed-bed reactor, the coolant temperature was set to 250°C; in the simulation of the monolithic reactor, however, T_{cool} was varied, being regarded as an optimization parameter as discussed below.

A preliminary sensitivity analysis was carried out on the individual design parameters of the monolith catalyst (ξ, λ, m and k_s), as well as on the coolant temperature, T_{cool}. As a general result, only the primary reaction (13) was found limited by intraporous diffusion, therefore, all the conditions resulting in reduced diffusional resistances imply a beneficial impact on the HCHO selectivity. For example, the selectivity was enhanced by monolith designs associated with a small catalyst volume fraction (ξ), i.e. with thin catalyst layers. Of course reducing ξ brings about also a reduction of the CH_3OH conversion; in the absence of diffusional limitations, however, this can be recovered by raising the coolant temperature, since higher temperatures do not favor the secondary reaction in this case. The selectivity was also improved by the following:

- Reducing the monolith pitch (m), since this grants greater geometric areas per unit monolith volume, eventually resulting in thinner washcoats for a given catalyst load.
- Incrementing the intrinsic conductivity (k_s) and the volume fraction (λ) of the support, so as to promote the removal of the reaction heat: in fact marked hot spots enhance locally the diffusional limitations on the main reaction, and reduce the overall HCHO selectivity; notice, however, that incrementing the volume fraction (λ) at constant m and ξ results in a greater washcoat thickness (δ_w), which may also eventually lower the catalyst effectiveness and the yield.

The calculated effect of the coolant temperature is shown in Fig. 1 for a set monolith design. Increasing T_{cool} enhances the CH_3OH conversion, but tends to decrease slightly the HCHO selectivity because of the negative effect associated with the enhanced diffusional resistances. Accordingly, the HCHO yield exhibits a maximum (93.4%) at $T_{cool} = 297$°C; this value is already very close to the best yield for the optimized packed-bed reactor reported in [10]. Notably, under the conditions of Fig. 1, the calculated temperature distributions were virtually flat throughout the reactor, with only modest axial gradients at the highest investigated T_{cool}.

With the intrinsic thermal conductivity of the monolith support (k_s) set to 200 W/(m K), representative of Al, and the monolith pitch (m) set to 2 mm, optimal values of the monolith volume fractions of metallic support (λ) and catalytic washcoat (ξ) and of the coolant temperature (T_{cool}) were searched with respect to the HCHO yield, taken as the objective function. The best result (yield = 97.2%, HCHO selectivity = 97.4%) were obtained with $\lambda = 0.1$, $\xi = 0.03$ (corresponding to washcoat thickness = 16 μm, wall thickness = 0.051 mm, channel opening = 1.9 mm) and $T_{cool} = 361$°C. Again, the corresponding axial profiles of catalyst temperature were essentially flat, with a maximum temperature increment ΔT_{max} of

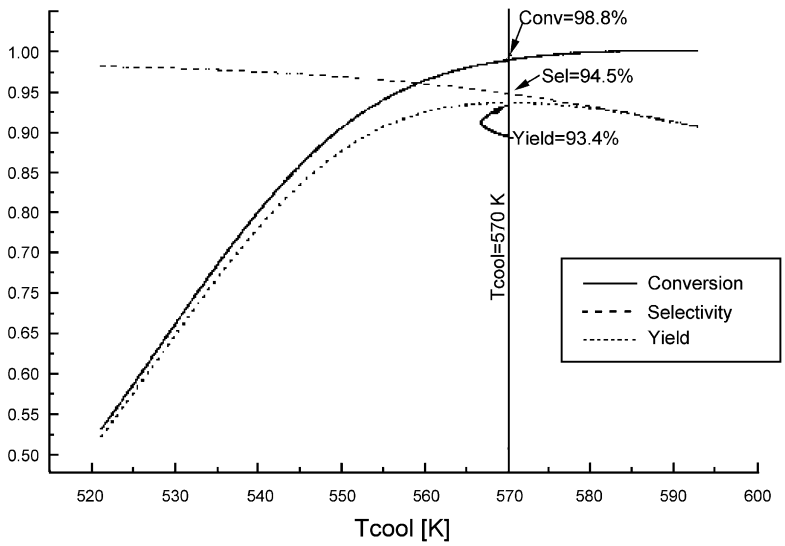

Fig. 1. Formaldehyde reactor. Effect of coolant temperature on CH_3OH conversion, HCHO selectivity and HCHO yield. Monolith configuration: $m = 2\,\text{mm}$, $\xi = 0.2$, $\lambda = 0.2$, $k_s = 70\,\text{W/(m K)}$.

7°C only. Such results appear significantly better than those reported in [10] for the optimized packed-bed reactor (yield = 93.6%, $\Delta T_{max} \approx 100$°C). The optimal performance of the monolith catalyst originates from: (i) a thin catalyst layer, which prevents diffusional limitations from adversely affecting the selectivity; (ii) a high level of T_{cool}, which increments the average reactor temperature and hence the overall CH_3OH conversion; (iii) a thickness of the highly conductive monolith walls adequate enough to grant near-isothermal operation, preventing hot-spot formation.

It should be emphasized that the increment of T_{cool} can be exploited to promote the CH_3OH conversion, and to compensate for the small volume fraction of active catalyst, because the process is operated essentially under kinetic control, and a higher temperature level does not adversely affect the selectivity according to the present kinetic scheme, where the activation energy of the consecutive undesired reaction is lower than that of the primary reaction.

Fig. 2 compares centerline axial profiles of the catalyst temperature for the optimized packed-bed reactor [10] and for optimized monolithic reactors with $k_s = 200$ and $70\,\text{W/(m K)}$. The drastic reduction of the temperature gradients is clearly apparent.

The optimization of the monolith reactor was carried out without introducing any constraint on the catalyst temperature. In fact, the computed optimal T_{cool} is over 100°C above the coolant temperature of the reference industrial packed-bed reactor, and even slightly greater than the maximum hot-spot temperature reported in [10]. Actually, the deactivation of the Fe_2O_3–MoO_3 catalyst can be strongly accelerated by high temperatures. Accordingly, alternative suboptimal configurations with lower levels of T_{cool} were investigated, too, with regard to the thermal stability of the catalyst. For given other catalyst parameter values, Fig. 3 presents a plot of the ξ–T_{cool} combinations affording HCHO yields in the range 94–96%, which are still superior to the performance of the industrial packed-bed reactor. Thus, excellent yields can be achieved even with temperature levels largely reduced as compared to the optimal T_{cool}. For a set coolant temperature, Fig. 3 shows that two different levels of ξ result in the same yield, the configuration with greater ξ corresponding to a greater CH_3OH conversion but to a lower HCHO selectivity. Practically isothermal conditions were estimated for all the reactor solutions included in Fig. 3. As an additional benefit, the pressure drop was limited to less than 1% of the inlet pressure versus the 10% pressure loss reported in [10] for the conventional packed-bed reactor.

Further simulations showed that a high (>95%) HCHO yield can be achieved also in the case of reactor

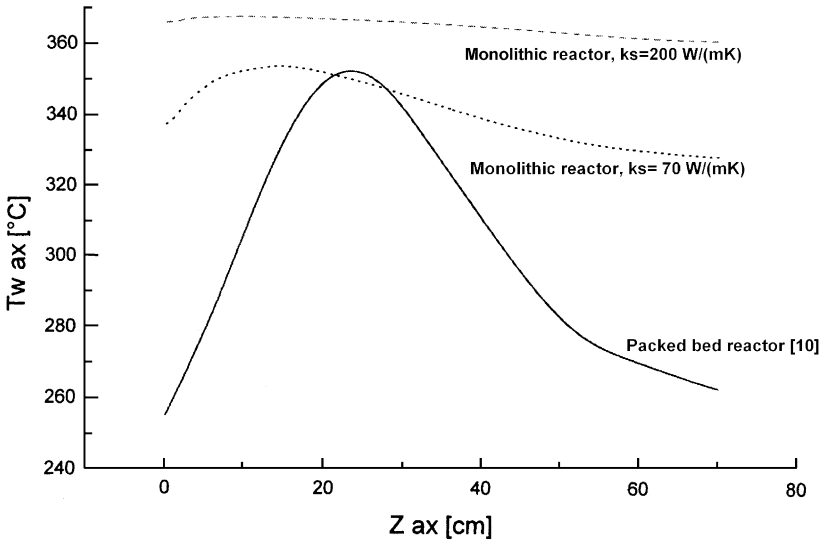

Fig. 2. Formaldehyde reactor. Axial catalyst temperature profiles for: (a) packed-bed reactor, $T_{cool} = 250°C$ (from Ref. [10]); (b) monolithic reactor, $k_s = 70\,W/(m\,K)$, $T_{cool} = 327°C$; (c) monolithic reactor, $k_s = 200\,W/(m\,K)$, $T_{cool} = 361°C$.

tubes with diameter incremented from 1 to 3 in., which would afford important savings in the reactor investment costs. However, the volume fraction of the Al monolith support had to be increased by a factor of 4 ($\lambda = 0.4$) to compensate for the greater heat transfer resistances.

3.2. Epoxidation of ethylene

In the production of ethylene oxide by selective oxidation of ethylene over industrial Ag-based catalysts, a major parasitic reaction is the total combustion of C_2H_4 (16) which occurs in parallel to the primary

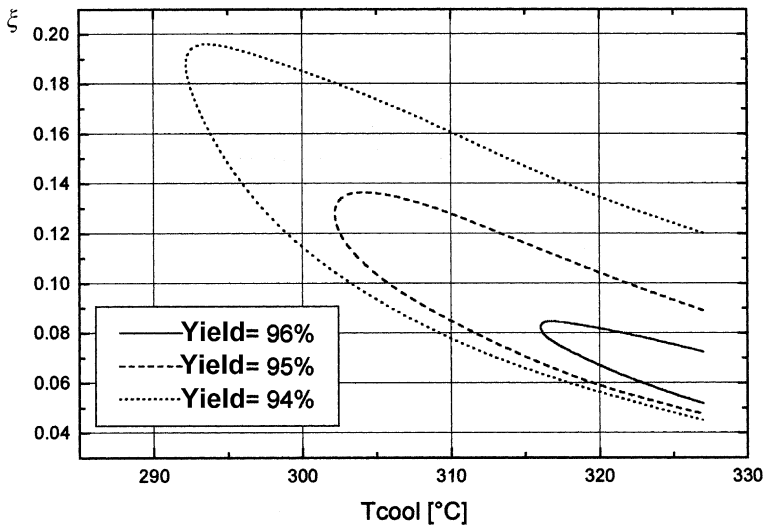

Fig. 3. Formaldehyde reactor. Combinations of ξ and T_{cool} affording HCHO yields in the range 94–96%. Other catalyst parameters: $\lambda = 0.1$, $m = 2\,mm$, $k_s = 200\,W/(m\,K)$.

Table 2
Simulation parameters for the industrial ethylene oxide reactor [14]

Reactor	
Tube length, L (m)	12
Tube inner diameter, D (m)	0.03925
Catalyst density, ρ_{cat} (kg/m^3)	1800
Operating conditions	
Mass velocity, W_t (kg/(m^2 s))	13.6
Coolant temperature, T_{cool} (°C)	250
Inlet temperature, T^0 (°C)	245
Inlet pressure, P^0 (atm)	20.2
Feed C_2H_4 mole fraction, $Y^0_{C_2H_4}$	0.174
Feed O_2 mole fraction, $Y^0_{O_2}$	0.073
Feed CO_2 mole fraction, $Y^0_{CO_2}$	0.115

reaction (15):

$$C_2H_4 + \tfrac{1}{2}O_2 \rightarrow C_2H_4O, \quad \Delta H_R = -25\,\text{kcal/mol} \tag{15}$$

$$C_2H_4 + 3O_2 \rightarrow 2CO_2 + 2H_2O, \quad \Delta H_R = -317\,\text{kcal/mol} \tag{16}$$

and is associated with a greater activation energy as compared to the epoxidation reaction. The overall process is a strongly exothermic one and poses serious problems of temperature control, essentially due to a selectivity to C_2H_4O limited to 70–80%. Accordingly, limitation of the hot spots is a critical issue. In fact, the use of "high conductivity" monolithic catalysts has been already proposed and theoretically investigated for this process [12], although for conditions different from those prevailing in current industrial operation. The interest in novel reactor solutions for the ethylene oxide process is also documented by a recent paper [13] discussing the application of a membrane reactor.

Table 3
Kinetic parameters for rate equations (17) (partial pressures in bar)

	R_{15}	R_{16}
k	8.7×10^6	1.2×10^{11}
T_{act} (K)	8800	12800
K^0_E (bar^{-1})	0.010	0.0021
$T_{ads,E}$ (K)	3000	3500
K_{O_2} (bar^{-1})	2.2	10.4
K_{CO_2} (bar^{-1})	24.0	89.0
K_w (bar^{-1})	50.0	40.0

As in the previous section, the purpose of the present work is to investigate the specific design of monolithic honeycomb catalysts for this process, which are suitable to minimize hot-spot temperatures by enhancing the heat transfer properties of the catalyst/reactor system.

Reference data for an industrial packed-bed reactor with silver catalyst operated within an oxygen-based process were taken from [14]. The relevant design and operating parameters are summarized in Table 2. Rate expressions for the two reactions (15) and (16) were adapted from literature sources [15–18] in order

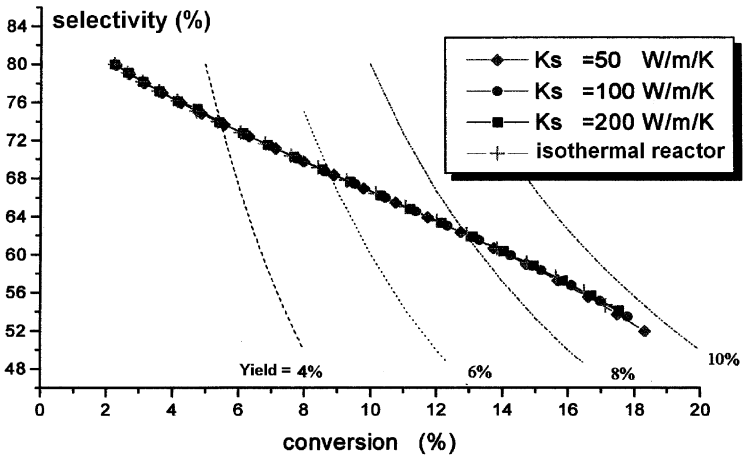

Fig. 4. Ethylene oxide reactor. Conversion–selectivity relationship for $k_s = 50$, 100 and 200 W/(m K), and comparison with ideal isothermal reactor. Other catalyst parameters: $\lambda = 0.2$, $\xi = 0.2$, $m = 2$ mm.

to properly account for a number of features associated with industrial operation of the process, including the kinetic effects of CO_2 and H_2O, the superatmospheric feed pressure, the addition of chlorinated compounds to the feed stream to moderate the combustion reactions. The rate equations are in the form

$$R_j = \frac{k_j K_{\mathrm{E},j} \sqrt{K_{\mathrm{O}_2,j}} P_{\mathrm{E}} \sqrt{P_{\mathrm{O}_2}}}{(1 + K_{\mathrm{E},j} P_{\mathrm{E}} + \sqrt{K_{\mathrm{O}_2,j}} \sqrt{P_{\mathrm{O}_2}} + K_{\mathrm{CO}_2,j} P_{\mathrm{CO}_2} + K_{\mathrm{w},j} P_{\mathrm{w}})^2} \quad (\mathrm{mol}/(\mathrm{cm}^3\,\mathrm{s})) \tag{17}$$

with $j = 15$ or 16, $k_j = k_j \exp(-T_{\mathrm{act},j}/T)$ and $K_{\mathrm{E},j} = K^0_{\mathrm{E},j} \exp(T_{\mathrm{ads,E},j}/T)$. Table 3 provides

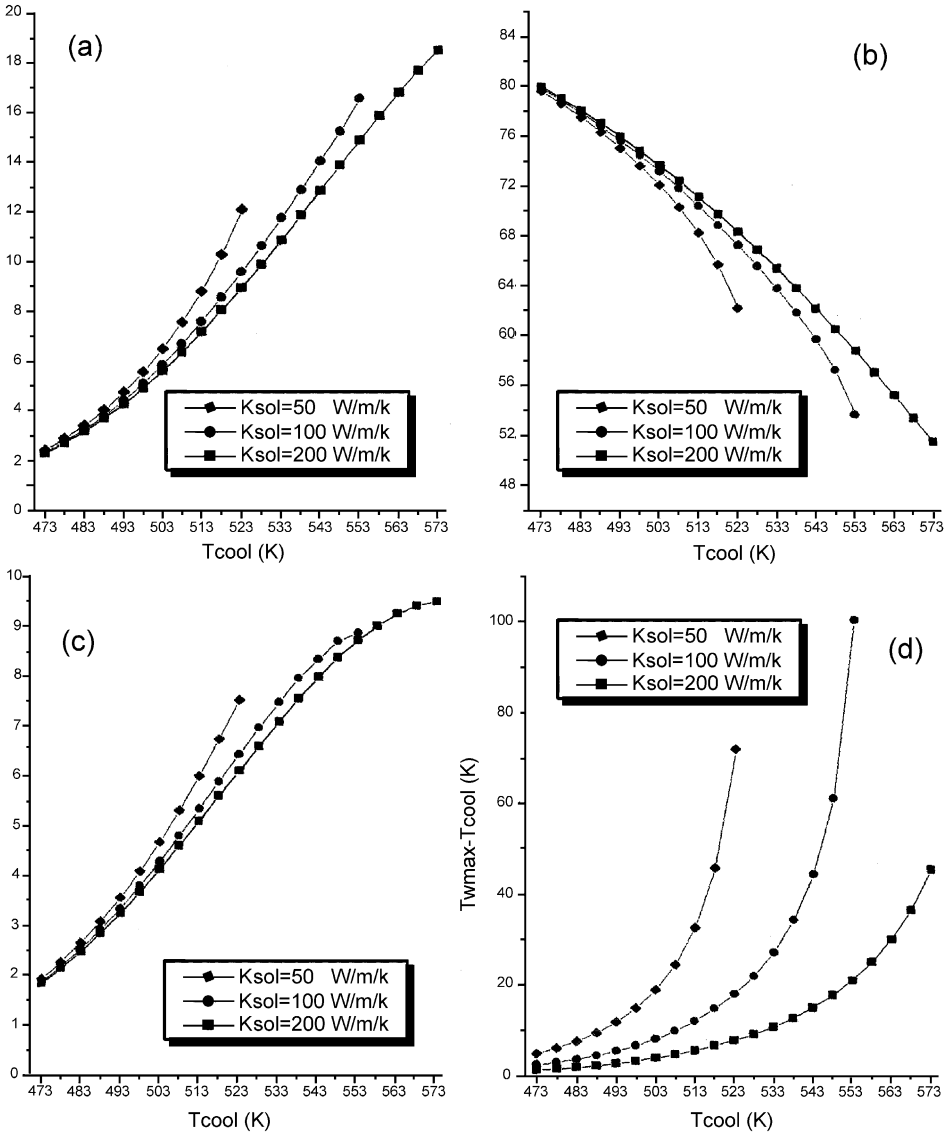

Fig. 5. Ethylene oxide reactor. Effects of T_{cool} and k_{s} on C_2H_4 conversion (a), ethylene oxide selectivity (b) and yield (c), hot-spot temperature (d). Other catalyst parameters: $\lambda = 0.05$, $\xi = 0.2$, $m = 2\,\mathrm{mm}$.

the rate parameter estimates. The rate expressions, Eq. (17), were checked against packed-bed reactor data reported in [19], and were eventually included in the model to simulate a multitubular reactor loaded with metallic honeycomb supports coated with Ag/α-Al_2O_3 washcoats, the goal being here the optimization of the selectivity to ethylene oxide.

The simulation results confirmed that isothermal operation is feasible also for the ethylene oxide reactor due to the excellent effective thermal conductivity of the metallic monoliths, provided that a reasonable volume fraction of support is adopted. For a monolith pitch $m = 2$ mm, and for monolith volume fractions of support (λ) and catalyst (ξ) both equal to 0.2, Fig. 4 shows that the reactor behavior is identical to that of an isothermal reactor for a variety of conditions, provided that the intrinsic thermal conductivity of the monolith support is equal to or greater than 50 W/(m K): under such conditions the conversion–selectivity relationship is governed uniquely by the intrinsic kinetics. Only upon reducing the support volume fraction down to 0.05, one notices the onset of significant temperature gradients at the highest C_2H_4 conversions for the low conductivity supports, with associated negative effects on the selectivity, as illustrated in Fig. 5. A reactor design based on larger tubes ($D = 76.2$ mm) was also found feasible at the expense of a greater volume fraction of catalyst support ($\lambda = 0.2$), but only with k_s greater than 100 W/(m K).

Notably, the selected values of ξ correspond in this case to a washcoat thickness in excess of 100 μm. Such values provide an adequate overall catalyst inventory. Even thicker catalyst layers would be desirable to increment the process yield, but the adhesion of thick washcoats onto metallic surfaces may be critical [20]. On the other hand, increments of the coolant temperature, as adopted for the formaldehyde reactor, are not compatible with the present kinetic scheme, since they would adversely affect the selectivity. For a fixed washcoat thickness (e.g. the greatest one compatible with adhesion requirements), the overall catalyst load can be incremented by reducing the monolith pitch. Assuming a 120 μm thick catalytic washcoat, calculations show that reducing the pitch to 1 mm would indeed effect significant improvements of conversion (from 8.5 to 14%) and yield (from 6 to 9%) with only a slight loss of selectivity. At this stage, the question is whether a honeycomb monolith made of highly conductive material ($k_s \geq 50$ W/(m K)) with such a geometry can be manufactured on an industrial scale at a reasonable cost.

4. Conclusions

The simulation results herein presented point out a number of potential advantages associated with running industrial selective oxidation processes in fixed-bed gas/solid reactors loaded with "high conductivity" monolith catalysts in the place of conventional catalyst pellets.

- The strong reduction of the pressure drop (down to less than 1%) is a significant benefit, especially for processes operating with partial conversions of the reactants and large recycle rates as in the ethylene oxide case.
- Virtually, isothermal operation of the fixed-bed reactor seems feasible upon properly selecting the design variables which affect the monolith thermal conductivity, namely the intrinsic conductivity and the volume fraction of the monolith matrix. The concept of an isothermal reactor behavior which avoids the hassles of fluidized beds is obviously quite attractive.
- The improvement of the effective radial thermal conductivity of the catalyst bed may be such as to afford a significant increment of the reactor tube diameter, with important economical benefits affecting the investment costs.

On the other hand, a couple of issues have been identified which require further development work:

1. In the investigated monoliths, the overall load of active catalyst per unit reactor volume (typically 0.05–0.2, v/v) is remarkably smaller than in conventional packed beds (typically 0.4–0.5, v/v). This limits the specific productivity of the reactor. Possible ways to overcome this problem include: (a) incrementing the washcoat thickness, which is, however, limited by adherence problems associated with the coating method and by the onset of diffusional limitations; (b) incrementing the specific surface area of the monolithic support by reducing its pitch, which is, however, limited by the manufacturing technologies; (c) incrementing the

catalyst activity by increasing the amount of active phase (or possibly reducing the feed concentration of moderating agent in the ethylene oxide reactor); (d) incrementing the coolant temperature, which is, however, acceptable only if a higher average temperature level is not detrimental to the process selectivity. Notably, the adoption of such remedies depends on the specific process characteristics: the increment of the coolant temperature was found feasible for the formaldehyde process, whereas resort to the increment of the washcoat thickness and to the reduction of the monolith pitch was necessary for the ethylene oxide process.

2. On enhancing the effective radial thermal conductivity of the catalyst bed, the controlling thermal resistance may become associated with the contact at the interface between the monolith catalyst and the internal reactor tube wall. This aspect has not been addressed in the present study. Heat transfer across such an interface could be optimized both by favoring an intimate contact between the surfaces and by incrementing the contact area, which, however, involves improvements in the geometry and configuration of the structured catalysts.

Due to the aspects above, additional work is required for developing practical "high conductivity" monolithic catalysts suitable for industrial applications. Such work shall be necessarily connected both with the manufacturing technologies of monolithic catalysts and with the specific features of the individual catalytic processes.

References

[1] G. Groppi, E. Tronconi, AIChE J. 42 (1996) 2382.
[2] G. Groppi, E. Tronconi, Chem. Eng. Sci. 55 (2000) 2161.
[3] G. Groppi, G. Airoldi, C. Cristiani, E. Tronconi, Catal. Today 60 (2000) 57.
[4] E. Tronconi, G. Groppi, Chem. Eng. Sci. 55 (2000) 6021.
[5] G. Groppi, A. Belloli, E. Tronconi, P. Forzatti, Chem. Eng. Sci. 50 (1995) 2705.
[6] G. Eigenberger, Chem. Eng. Sci. 27 (1972) 1917.
[7] B. Finlayson, Nonlinear Analysis in Chemical Engineering, McGraw-Hill, New York, 1980.
[8] W.H. Press, S.A. Teukolsky, W.T. Vetterling, B.P. Flannery, Numerical Recipes in FORTRAN, 2nd Edition, Cambridge University Press, Cambridge, 1992, p. 774.
[9] T.C. Wayburn, J.D. Seader, Comput. Chem. Eng. 11 (1987) 7.
[10] W.H. Ray, L.C. Windes, M.J. Schwedock, Chem. Eng. Commun. 78 (1989) 1.
[11] M. Dente, A. Collina, I. Pasquon, La Chimica e l'Industria 46 (1964) 1326.
[12] V. Ragaini, G. De Luca, B. Ferrario, P. Della Porta, Chem. Eng. Sci. 35 (1980) 2311.
[13] D. Lafarga, A. Varma, Chem. Eng. Sci. 55 (2000) 749.
[14] N. Piccinini, G. Levy, Can. J. Chem. Eng. 62 (1984) 541.
[15] P.C. Borman, K.R. Westerterp, Ind. Eng. Chem. Res. 34 (1995) 49.
[16] E.P.S. Schouten, P.C. Borman, K.R. Westerterp, Chem. Eng. Process. 35 (1996) 43.
[17] E.P.S. Schouten, P.C. Borman, K.R. Westerterp, Chem. Eng. Process. 35 (1996) 107.
[18] P. Kripylo, L. Moegling, D. Klose, H. Sueptitz, Chem. Technol. 34 (1982) 85.
[19] I. Simiceanu, I. Todea, M. Stanca, A. Pop, Studia Univ. Babes-Bolyai, Series Chemia 34 (1989) 3.
[20] M. Valentini, G. Groppi, C. Cristiani, M. Levi, E. Tronconi, P. Forzatti, Catal. Today 69 (2001) 307.